

Original research articles

Research on microseismic denoising method based on CBDNet

Jianchao Lin, Jing Zheng*, Dewei Li, Zhixiang Wu

China University of Mining and Technology (Beijing), Beijing, 10083, China

State Key Laboratory of Coal Resources and Safe Mining, Beijing, 10083, China



ARTICLE INFO

Keywords:

Denoising
Microseismic
Deep learning
Surface monitoring

ABSTRACT

Noise suppression is an important part of microseismic monitoring technology. Signal and noise can be separated by denoising and filtering to improve the subsequent analysis. In this paper, we propose a new denoising method based on convolutional blind denoising network (CBDNet). The method is partially modified for image denoising network CBDNet to make it suitable for one-dimensional data denoising. At present, most of the existing filtering methods are proposed for the Gaussian white noise denoising. In contrast, the proposed method also learns the wind noise, construction noise, traffic noise and mixed noise through the strategy of residual learning. The full convolution subnetwork is used to estimate the noise level, which significantly improves the signal-to-noise ratio and its performance of removing the correlated noise. The model is trained with different types of real noise and random noise. The denoising result is evaluated by corresponding indexes and compared with other denoising methods. The results show that the proposed method has better denoising performance than traditional methods, and it has a superior noise suppression level for oil well construction noise and mixed noise. The proposed method can suppress the interference of time-frequency overlapped end to end and still have noise suppression and event detection capability even if the signal is superimposed on other types of noise.

1. Introduction

Microseismic monitoring technology can be used in unconventional oil and gas development, mine disaster monitoring, CO₂ capture, utilization and storage (CCUS) and other fields. For microseismic monitoring technology, denoising is an important part of its data processing technology (Dai et al., 2019). Because the amplitude of the microseismic (small magnitude) signals is always much weaker than that of seismic signals, and the measured data is always polluted by noise, the signal-to-noise ratio (SNR) is much lower than that of active source seismic events. It is difficult to directly pick up arrive time and locate events from the original observation data.

In order to suppress noise and improve the accuracy of arrival time picking and localization, many efforts have been made to develop many effective denoising methods. Traditional microseismic noise suppression methods are proposed based on domain transform algorithms and some thresholding methods, including wavelet transform (Cao and Chen, 2005; Gaci, 2014; Liu et al., 2016; Mousavi et al., 2016; Mousavi and Langston, 2017), continuous wavelet transform (CWT) (Mousavi and Langston, 2016b,a), short time Fourier transform (STFT) (Allen and Rabiner, 1977), S-transform (Tselentis et al., 2012), radon transform (Sabbione et al., 2013, 2015; Zhang et al., 2015), wavelet packet

transform (WPT) (Galiana-Merino et al., 2003; Shuchong and Xun, 2015), meander transform (Neelamani et al., 2008), empirical mode decomposition (EMD) (Liu et al., 2014; Bekara and Baan, 2009; Chen et al., 2016; Han and Baan, 2015) and so on.

In recent years, denoising methods based on deep learning have been gradually applied to microseismic data processing. Among them, the most widely used denoising method for microseismic data is filtering based on convolution neural network (CNN) (Li et al., 2018; Liu et al., 2021; Mandelli et al., 2019; Liu et al., 2018; Si and Yuan, 2018; Kim et al., 2019). In addition, denoising convolutional neural network (DnCNN) (Zhang et al., 2017) and convolutional networks for biomedical image segmentation (U-Net) (Ronneberger et al., 2015) were first used for image denoising and image segmentation tasks, in which DnCNN used end-to-end neural network models to reduce Additive White Gaussian Noise (AWGN), and for the first time used residual learning strategy in the field of image reconstruction. Then, some researchers applied structures based on DnCNN and U-Net to seismic data processing, including but not limited to denoising and seismic phase identification.

Zhu et al. (2019) made some adjustments and improvements in the network structure and training strategy, taking the seismic signal

* Corresponding author at: China University of Mining and Technology (Beijing), Beijing, 10083, China.
E-mail address: jing@cumtb.edu.cn (J. Zheng).

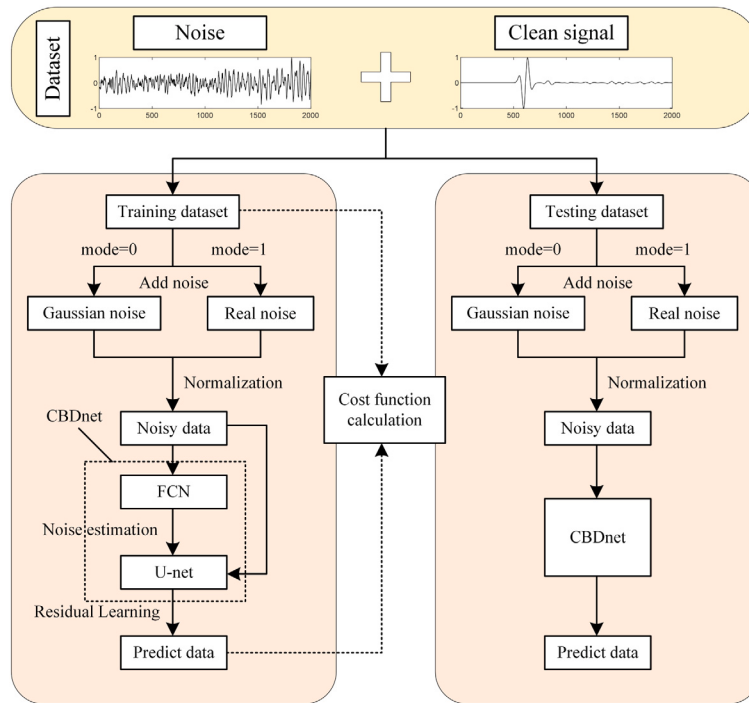


Fig. 1. Framework of the proposed method to attenuate microseismic noise.

after STFT as the input, and then decomposing the input data into signal and noise by the mask determined by the network. Zhang et al. (2020) applied the denoising method based on multi-layer U-Net neural network to the denoising of microseismic data. By learning the sparse characteristics in the time domain and frequency domain at the same time, as well as the mask correlation mapping function for signal separation, it can work well when the noise and signal frequency bands are similar. Zheng et al. (2021) built an end-to-end noise residual learning network through DnCNN, making it more timely in microseismic data denoising.

At present, in the field of microseismic denoising, most of the denoising methods based on deep learning are proposed for Gaussian white noise. When these methods encounter more complex real noise, the denoising performance is often greatly reduced. Therefore, we propose a microseismic denoising method based on convolutional blind denoising network (CBDNet). Compared with DnCNN network, an input noise intensity parameter σ is added to this network, and a full convolutional network is added to learn this parameter, so as to better adapt to different types of real noise.

The structure of this paper is as follows. Firstly, the proposed denoising method and its principle are introduced. Next, the performance of the denoising network is verified through experiments, and the denoising performance of the network for different types of noise is analyzed and compared with the traditional single-channel denoising method. The CBDNet used in training can be seen in the image processing network at the earliest (Guo et al., 2019), which will be adjusted and improved according to the prior information of microseismic signals.

2. Methods and network training

2.1. Methods

Single-channel microseismic data can be regarded as the superposition of effective signal and noise.

$$y = s + n \quad (1)$$

y represents the real microseismic data, s represents the signal to be extracted, and n represents the noisy data except the effective signal.

The feedforward process of deep convolution neural network can be expressed by Eq. (2).

$$y_{\text{out}} = f_{\theta}(x_{\text{in}}) \quad (2)$$

y_{out} is the output of the network, θ represents the parameters of the network, and f represents a nonlinear generating network that maps x_{in} to y_{out} . x_{in} is the network input after preprocessing.

$$x_{\text{in}} = (y - \text{mean}(y)) / (\text{max}(y) - \text{min}(y)) \quad (3)$$

With the supervised learning method and different learning strategies (waveform learning, noise residual learning), the network can be expressed into the following Eq. (4) (5).

$$\hat{x} = f_{\theta_1}(y) \quad \theta_1 = \arg \min_{\theta} \text{loss}(\hat{x}, x) \quad (4)$$

$$\hat{n} = f_{\theta_2}(y) \quad \theta_2 = \arg \min_{\theta} \text{loss}(y - \hat{n}, x) \quad (5)$$

\hat{x} represents the distribution of effective signals predicted by the network. \hat{n} represents the distribution of noisy signals predicted by the network. θ_1, θ_2 finds the best network parameters for minimizing the loss function. The mean square error is used to constrain the difference between the target signal and the estimated signal. The formula is as follows:

$$\text{loss}(y_{\text{out}}, y_{\text{label}}) = \|f_{\theta}(x_{\text{in}}) - y_{\text{label}}\|^2 \quad (6)$$

y_{label} is the label data produced.

The microseismic denoising network proposed in this paper is inspired by the image denoising network CBDNet (Guo et al., 2019), on the basis of which relevant improvements are made. The whole network can be divided into two subnetworks. One is the noise estimation subnetwork, which is a 3-layer fully convolutional networks (FCN) structure to learn the value of noise estimation. The second is the denoising subnetwork, which is a 9-layer U-Net structure. The input of the subnetwork is the output of the noise estimation subnetwork and the noisy-signal. The denoising subnetwork adopts the noise residual learning strategy, and the network learns noise instead of signal. Moreover, the network deals with one-dimensional signals, so the two-dimensional convolution operation is converted into one-dimensional

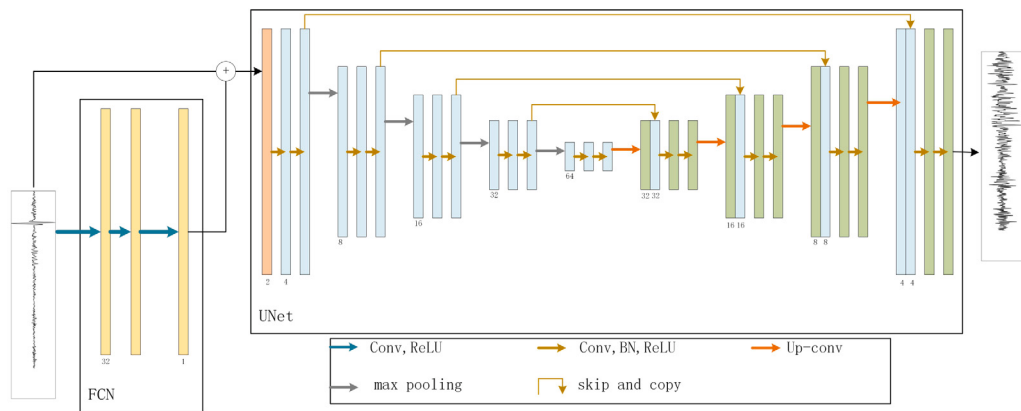


Fig. 2. Architecture of the proposed model.

convolution operation. The denoising processing framework is shown in (Fig. 1). (Fig. 2) shows the network architecture.

In the original CBDNet, its loss function is mainly composed of three parts. This paper has adjusted the details of its parameters. The overall formula of the original network loss function is shown below.

$$L = L_{\text{rec}} + \lambda_{\text{asymm}} L_{\text{asymm}} + \lambda_{TV} L_{TV} \quad (7)$$

L_{rec} is used to measure an error of the reconstructed signal of the denoising subnetwork, which is represented by the mean square error:

$$L_1 = \|(\mathbf{y} - \hat{\mathbf{y}}) - \mathbf{x}\|_2^2 \quad (8)$$

Where \mathbf{y} is the noisy-signal, $\hat{\mathbf{y}}$ is the noisy data predicted by the denoising subnetwork, and \mathbf{x} is the clean microseismic signal.

L_{asymm} , L_{TV} is used to constrain the noise estimation subnetwork, L_{asymm} is the constructed asymmetric loss to avoid the low noise characteristics of the output of the noise estimation subnetwork.

$$L_{\text{asymm}} = \sum_i |\alpha - \mathbb{I}_{(\hat{\sigma}(y_i) - \sigma(y_i)) < 0} | \cdot (\hat{\sigma}(y_i) - \sigma(y_i))^2 \quad (9)$$

Where $\hat{\sigma}(y_i)$ is the estimated noise level of the subnetwork, and $\sigma(y_i)$ is the real noise value. When $e < 0$, $\mathbb{I}_e = 1$. Otherwise, it is 0, and α is the set penalty.

L_{TV} is a regularization term introduced to constrain the rate of change of noise features. The detailed calculation formula is as follows:

$$L_{TV} = \|\nabla \hat{\sigma}(y)\|_2^2 \quad (10)$$

Where, $\nabla \hat{\sigma}(y)$ represents the gradient change of features. The original CBDNet is aimed at image denoising and needs to constrain the gradient change of noise features in both the height and width directions. This paper mainly focuses on one-dimensional microseismic signals, so there is only one constraint term.

2.2. Network training

The high SNR microseismic signals were acquired using forward simulation, setting a sampling window of 1.5 s, a sampling interval of 0.3 ms, a total of 5000 sampling points, and intercepting 2000 sampling points with signals as the length of the input signal. Data enhancement was carried out by adding Gaussian noise with different signal-to-noise ratios, wind noise from field acquisition, construction noise, traffic noise and mixed noise to the signals respectively. As the real noisy signals do not exactly satisfy the characteristics of Gaussian distribution and are more relevant to the situation in the field, the generalization ability of the network can be improved. A total of 300,000 training samples were constructed, with 20% of the samples used as a validation

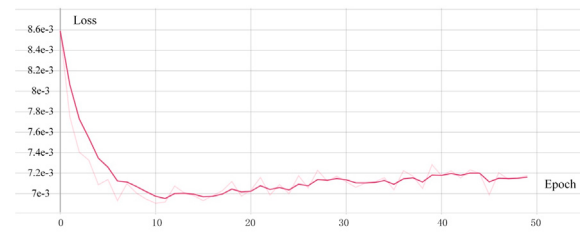
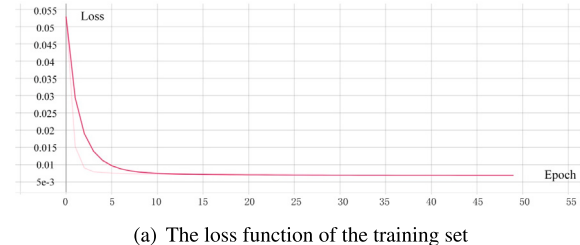


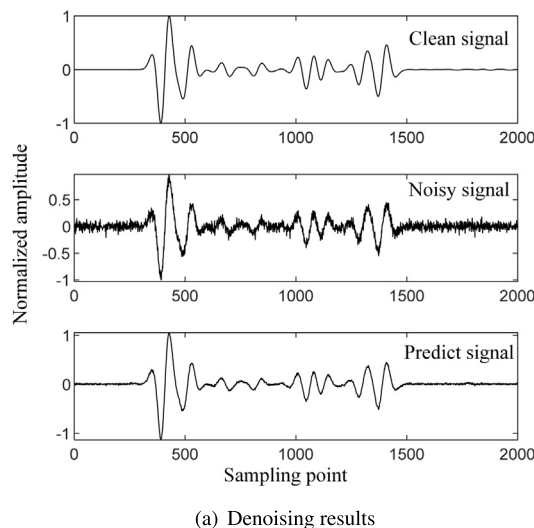
Fig. 3. Loss function.

set to determine hyperparameters and prevent the network from being overfitted for best results, 20% as a test set to evaluate the performance of the network, and the rest as a training set. The network was trained on an NVIDIA Tesla V100 GPU using the Adam optimizer with a learning rate of 0.0001 and a min-batch size of 128. (Fig. 3) shows the change of the loss function for each epoch of the training set and the validation set.

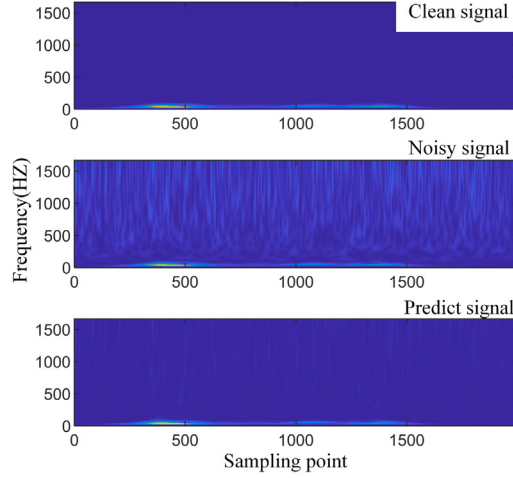
3. Results

3.1. Synthetic tests results

Compared with indoor or urban environment, the ambient noise at the oilfield site is more complex and has different intensity and frequency. In order to improve the denoising effect of deep learning denoising in the face of field noise, in addition to Gaussian random noise, a large number of wind noise, construction noise, traffic noise and mixed noise including multiple noise are added to the data set. The noisy signal was formed by superimposing the clean signal with noise. We get clean signal through forward simulation, and the noise includes Gaussian random noise and real noise. The denoising results of some noisy data selected from the test data set are shown in Figs. 4 to 8. It can



(a) Denoising results

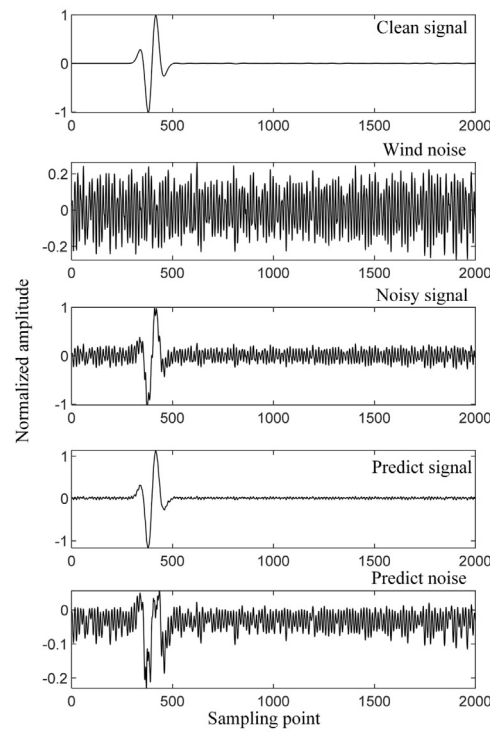


(b) Results in the time-frequency domain

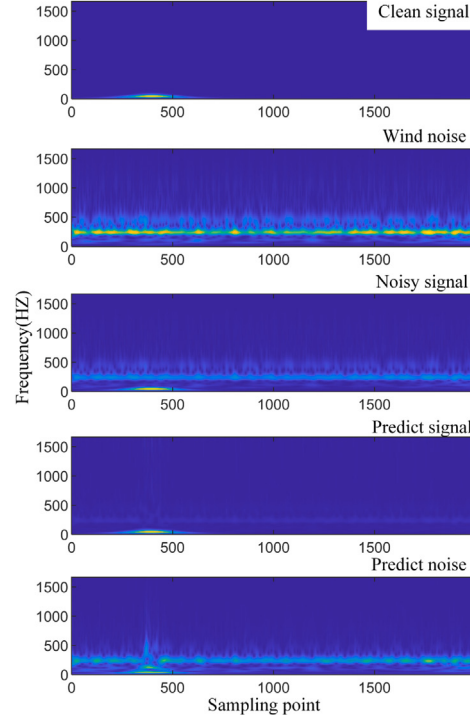
Fig. 4. Denoising results with Gaussian random noise.

be observed that the proposed method can successfully separate noisy data with different characteristics into estimated signals and estimated noise.

The proposed method has good denoising performance for microseismic signals with noise which have different types and different intensities. Wherein, the noisy signal in Fig. 4(a) is the microseismic signal with Gaussian random noise, and Fig. 4(b) is the corresponding time-frequency domain signal; Fig. 5 shows the noisy signal after adding the real wind noise from the field. Fig. 6 shows the noisy signal added with the real construction noise; Fig. 7 shows the noisy signal added with the real traffic noise; The noise added in Fig. 8 is a mixture of various ambient noise, including construction noise, traffic noise, wind noise, etc. (hereinafter referred to as mixed noise), which is more complex than a single type of real noise. The algorithm can restore the denoised signal with high accuracy, and can well suppress the Gaussian random noise and various types of practical noise commonly seen in field construction. The shape and amplitude characteristics of the predicted signal have also obtained high similarity fidelity. In addition, since the training set adopts a large amount of real noise, the proposed method has high applicability to the field data that need to be preprocessed.



(a) Denoising results

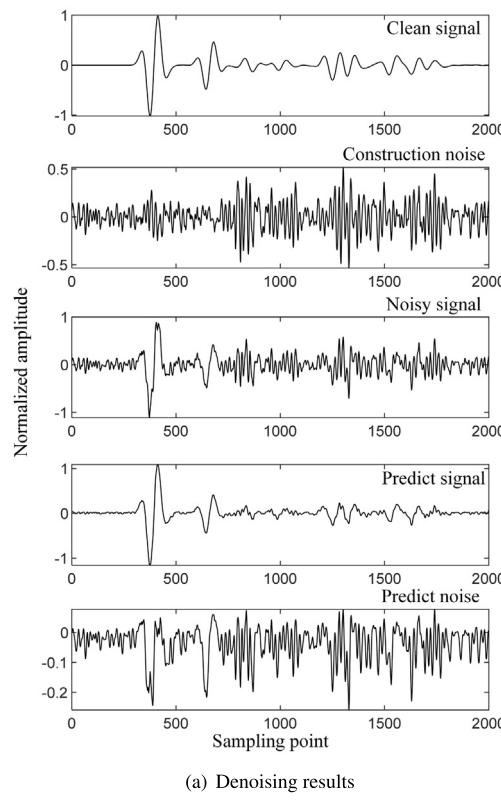


(b) Results in the time-frequency domain

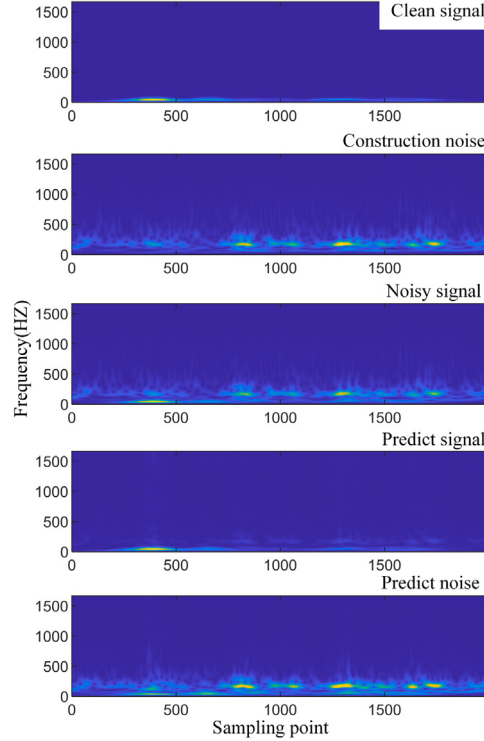
Fig. 5. Denoising results with real wind noise.

3.2. Analysis of test results

After the network training is completed, in order to verify the denoising effect, some indicators for evaluating the denoising performance are also needed for analysis, and we mainly analyzes the effect before and after denoising through three indicators: SNR, mean square

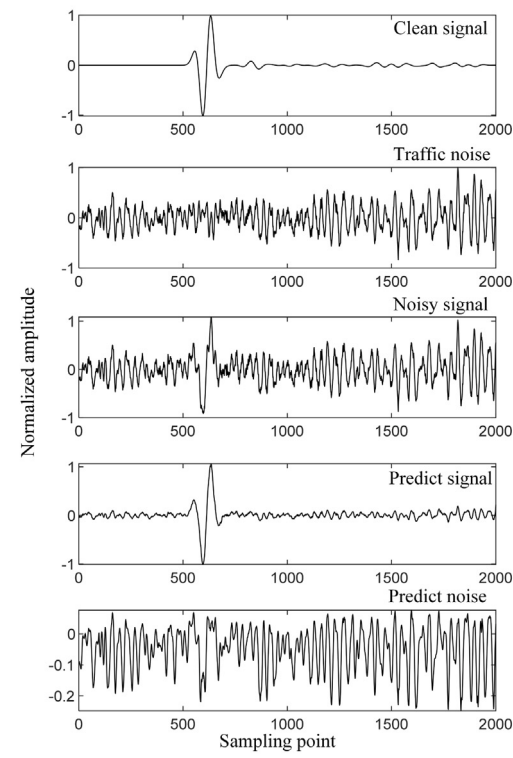


(a) Denoising results

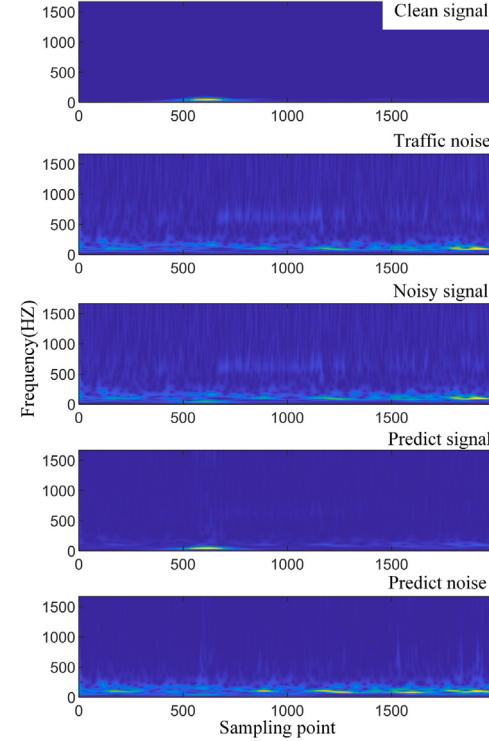


(b) Results in the time-frequency domain

Fig. 6. Denoising results with real construction noise.



(a) Denoising results



(b) Results in the time-frequency domain

Fig. 7. Denoising results with real traffic noise.

error (MSE) and similarity coefficient (R), as shown in Eqs. (11) to (13).

$$\text{SNR} = 10 \log_{10} \left(\frac{P_S}{P_n} \right) = 20 \log_{10} \left(\frac{A_s}{A_n} \right) \quad (11)$$

where P_S is the signal power, P_n is the noise power, A_s is the signal amplitude, and A_n is the noise amplitude.

$$\text{MSE} = \frac{\sum_{i=1}^n [f(x_i) - y_i]^2}{n} \quad (12)$$

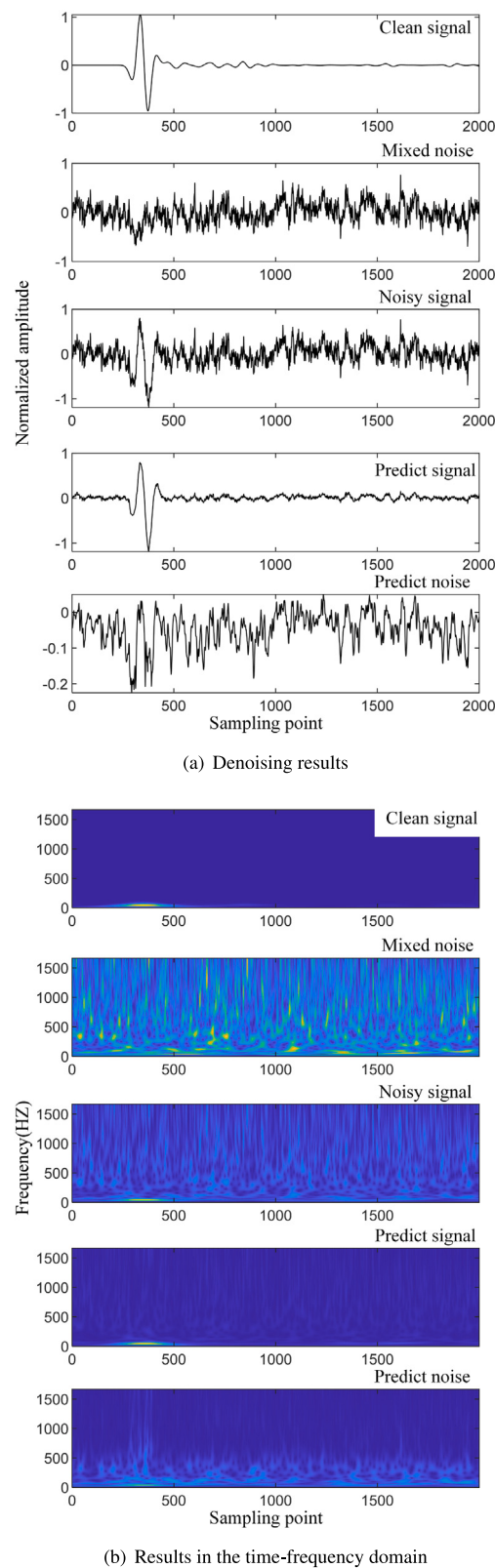


Fig. 8. Denoising results with real mixed noise.

where y_i is the true value of each sample, $f(x_i)$ is the predicted value of each sample, and n is the sample length.

$$R = \frac{\text{cov}(s, \hat{s})}{\sigma_s \times \sigma_{\hat{s}}} \quad (13)$$

where s is the original data and \hat{s} is the denoising data.

The denoising performance of the network can be well evaluated by using SNR, mean square error and similarity coefficient. As shown in Fig. 9(a), which is the histogram of the SNR distribution before and after denoising the noisy signal of some test sets. The average SNR of the input noisy signal is about 5.576 dB, and the average SNR after denoising treatment reaches about 13.814 dB, an average increase of about 8.238 dB, and an increase of about 147.8%. The mean square error of denoising is 0.04, and the average similarity coefficient reaches 0.95, which shows that the proposed method has a better denoising performance.

The method achieve a good denoising performance for randomly generated Gaussian random noise with different SNR. As shown in Fig. 9(b), it is the data containing Gaussian random noise. The average SNR of the input noisy signal is about 7.189 db. After denoising, the average SNR reaches about 16.287 db, with an average increase of about 9.098 db. Fig. 9(c) shows the data with wind noise. After denoising, the average SNR is increased by 5.997 db. Because of the higher complexity of real noise, compared with the Gaussian random noise, the denoising performance of the network for the real wind noise is relatively weak. Fig. 9(d) shows the data containing oil well construction noise. After noise removal, the average SNR has increased by 8.610 db. It is higher than the average performance of various noise except the Gaussian random noise, indicating that the network has a good denoising performance for oil well construction noise. Fig. 9(e) shows the data with traffic noise. It can be found that the SNR is increased by 5.810 db on average through denoising. Therefore, the ability of the network to reduce traffic noise is relatively weak, which is lower than the average performance of denoising. Fig. 9(f) shows the data with real mixed noise, and the average SNR is about 7.445 db higher. Compared with various types of real noise, the denoising performance of the proposed method for mixed noise is higher than that of wind noise and traffic noise, and lower than that of construction noise.

In practical engineering, the real noise often does not obey the Gaussian distribution, which will increase the difficulty of denoising. In this paper, microseismic signals containing different types of real noise are added to the training set to improve the denoising performance. Through comparison of evaluation indexes, it is concluded that the method performs well in removing Gaussian noise, oil well construction noise and mixed noise. In addition, it has certain denoising performance for wind noise and traffic noise. The denoising method has superior adaptability in the face of the common noise in practical engineering.

4. Comparison with other methods

4.1. Synthetic data

In order to further verify the denoising performance of the proposed method, we compared the proposed denoising method based on CBD-Net with the ensemble empirical modal decomposition (EEMD) and wavelet threshold transform (WT) denoising methods. Among them, sym8 wavelet base, 5-layer wavelet decomposition and fixed threshold calculation are selected in the wavelet threshold transformation. As shown in Figs. 10, three indicators are used to compare the denoising performance of the three filtering methods: SNR, similarity coefficient and mean square error of noisy signals and estimated signals.

By comparing Figs. 10(a) and 10(b), it can be seen that although the proposed denoising method is better to EEMD filtering and WT filtering in terms of the denoising performance of Gaussian random noise, the noise suppression levels of the three filtering methods are relatively close when the original SNR is high, that is, when the signal is relatively high quality. However, in the face of more complex and changeable real noise, the proposed method achieves a better denoising performance than EEMD filter and WT filter.

Compared with EEMD filtering and wavelet threshold transform filtering, the proposed method has the largest improvement in SNR,

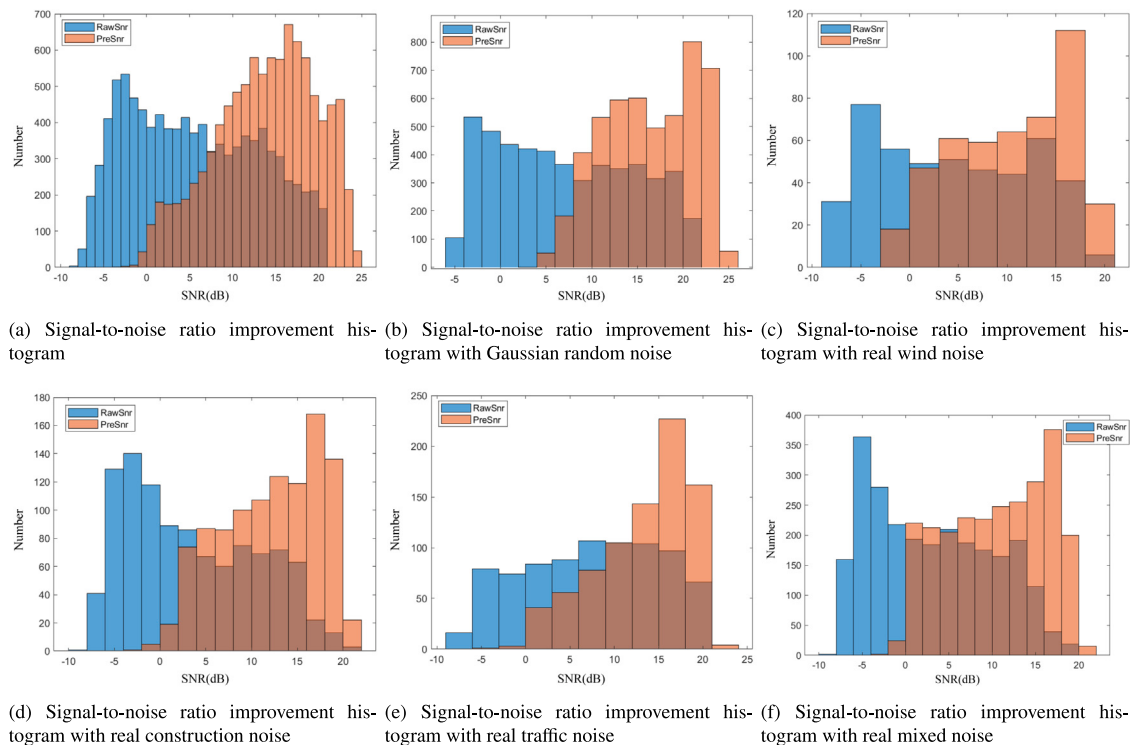


Fig. 9. Signal-to-noise ratio distribution of signals before and after denoising.

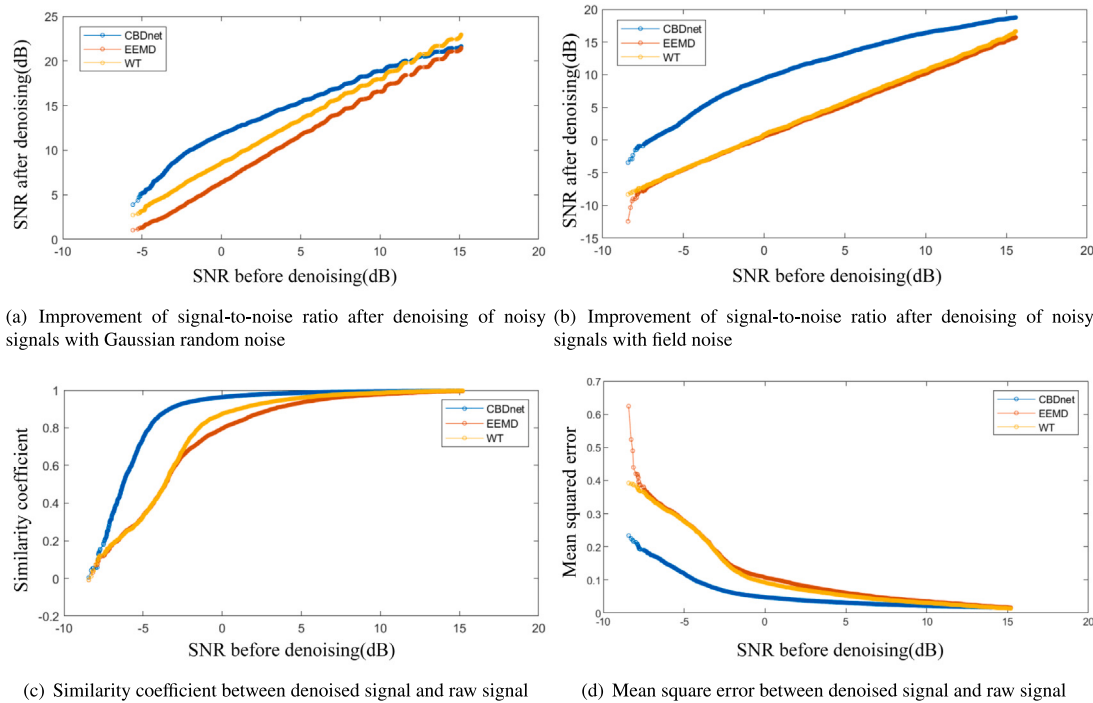


Fig. 10. Comparison of the denoising performance of empirical mode decomposition filter, wavelet threshold transform filter and proposed method.

which is much higher than the traditional denoising method, with an average increase of 8.238 db. The average EEMD filtering is about 3.288 db higher, and the average WT filtering is about 4.432 db higher. As shown in Figs. 10(c) and 10(d), the average similarity coefficient

of EEMD filtering is about 0.83, and the average mean square error is about 0.09; The average similarity coefficient of wavelet threshold transform filtering is about 0.86, and the average mean square error is about 0.08. Since the average similarity coefficient of the proposed

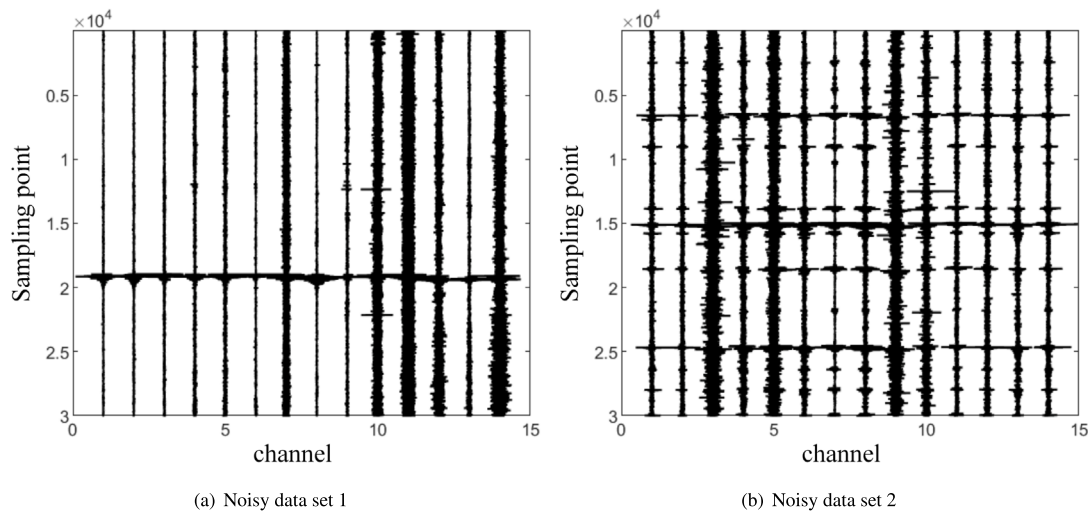


Fig. 11. Raw noisy field data set.

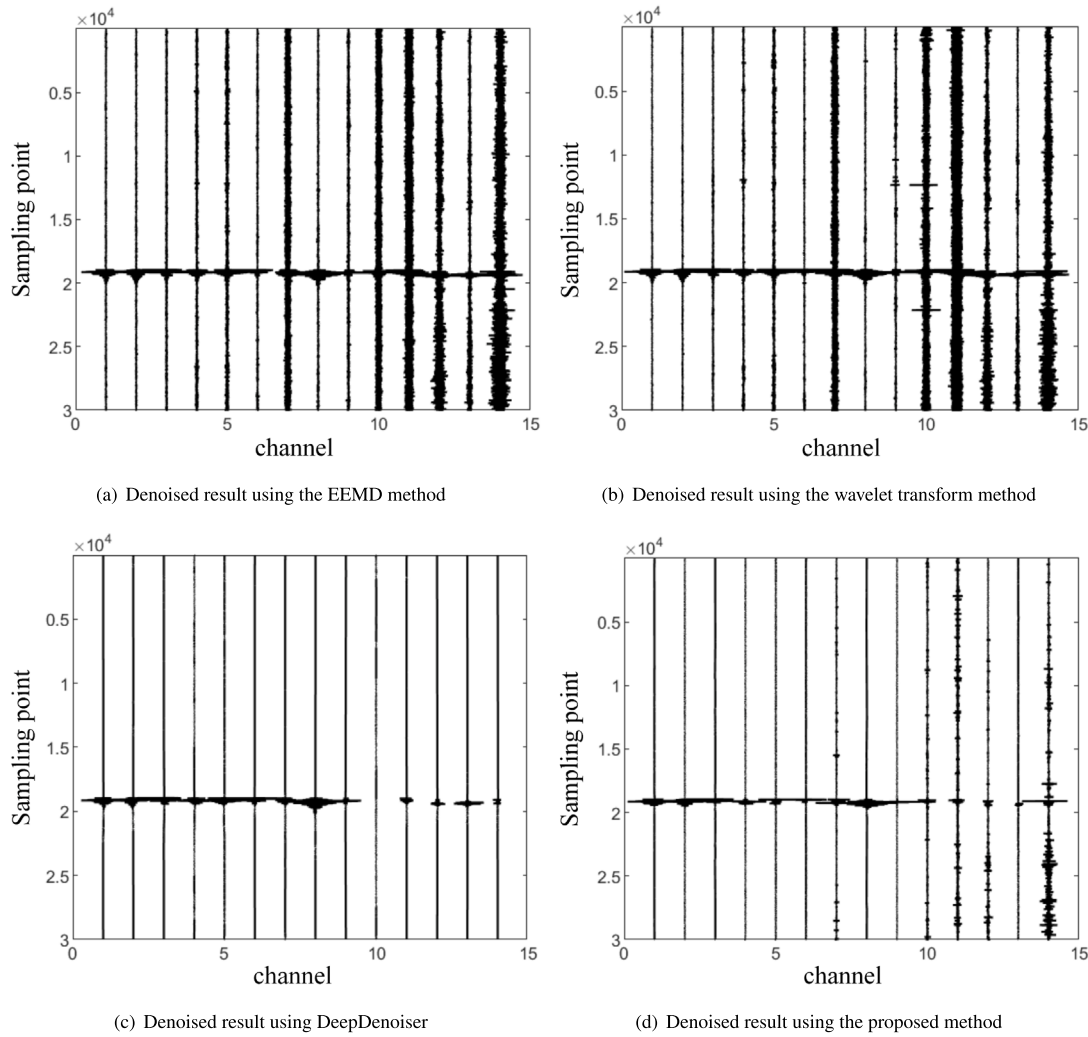


Fig. 12. Denoising comparison for different methods on field data 1.

method is higher than that of the two traditional methods, and the average mean square error is lower than that of the EEMD filter and WT filter, it can be seen that the denoising performance of the wavelet

threshold transform filter is slightly higher than that of the ensemble empirical mode decomposition filter method, but it is not as good as that of the CBDNet based denoising method.

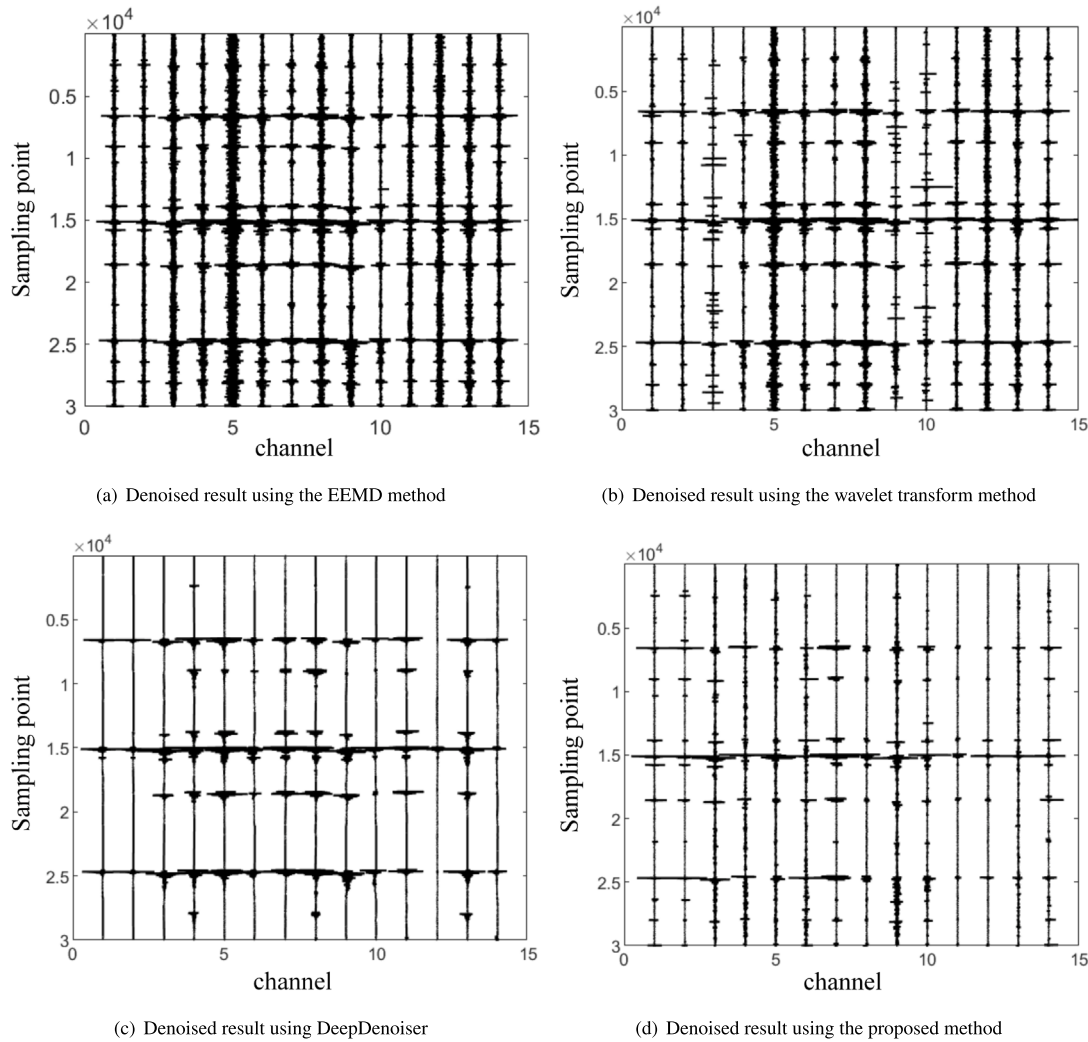


Fig. 13. Denoising comparison for different methods on field data 2.

4.2. Field data

In addition to applying the network to synthetic data, we still need to verify its denoising performance for real data. Therefore, two sets of field data are used as denoising examples, one with a single microseismic event and the other with multiple microseismic events.

As shown in Figs. 11, the noisy data set 1 were collected in Shizhuang Town, Qinshui County, Jincheng City, Shanxi Province. And the noisy data set 2 were collected in Mabi Town, Anze County, Linfen City, Shanxi Province. Figs. 12 and 13 show the denoised results using four different methods. Figs. 14 and 15 are the detailed denoising waveforms of the field data in the corresponding areas. We compare the proposed method with a deep neural networks-based method named DeepDenoiser, which can properly handles a variety of colored noise and non-earthquake signals (Zhu et al., 2019). Comparing the four denoising methods, the EEMD method has the weakest denoising performance can be shown clearly. The WT method can remove partial noise but the improvement of SNR is limited. Although DeepDenoiser has more noise suppression than the proposed method, the proposed method can retain more waveform details and each event can be picked up more precisely. Although the field data acquisition area and ambient noise are different, the proposed method can clearly separate the signal

and noise from the data. Therefore, the proposed method has better denoising performance than traditional denoising method, and has advantages over other deep learning methods.

5. Conclusions

We propose a microseismic signal processing method based on CBDNet neural network which is mainly for denoising of the surface microseismic monitoring. Different from other common deep learning methods, the proposed method simultaneously learns the Gaussian random noise, wind noise, construction noise, traffic noise and mixed noise through the residual learning strategy, which can significantly improve the SNR, and has better universality and signal authenticity. When encountering different types and different intensities of ambient noise in field work, even if the signal and noise are superposed, the proposed method can still suppress certain noise and extract the signal, and the denoising performance will be different when facing different types of noise.

The results show that the proposed method performs well in removing oil well construction noise and mixed noise, while the denoising performance for wind noise and traffic noise is relatively weak. But both can better extract the waveform characteristics of microseismic

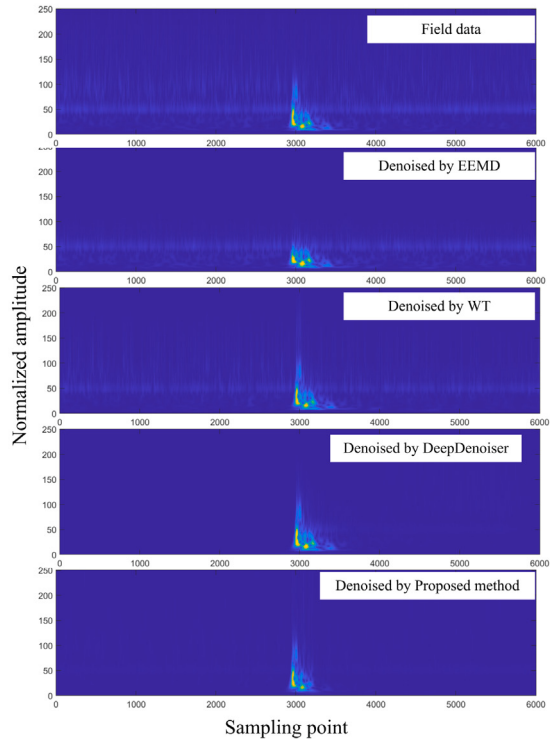
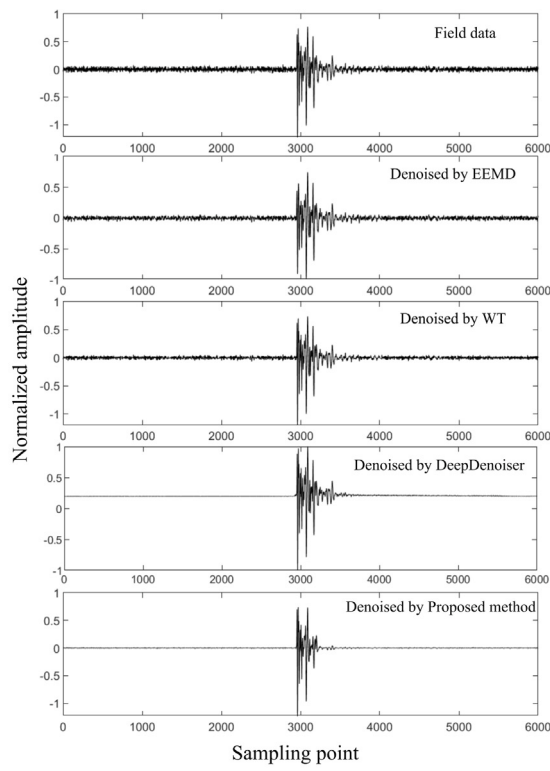


Fig. 14. The waveforms cut from the denoising results for data set 1.

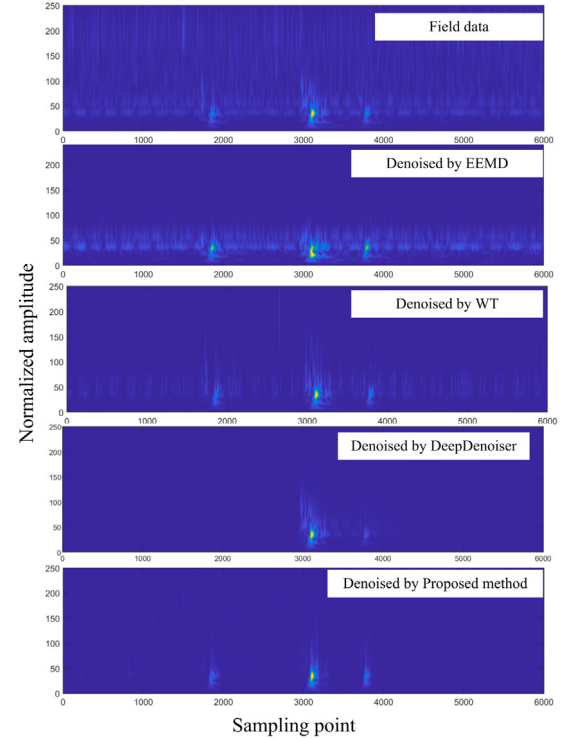
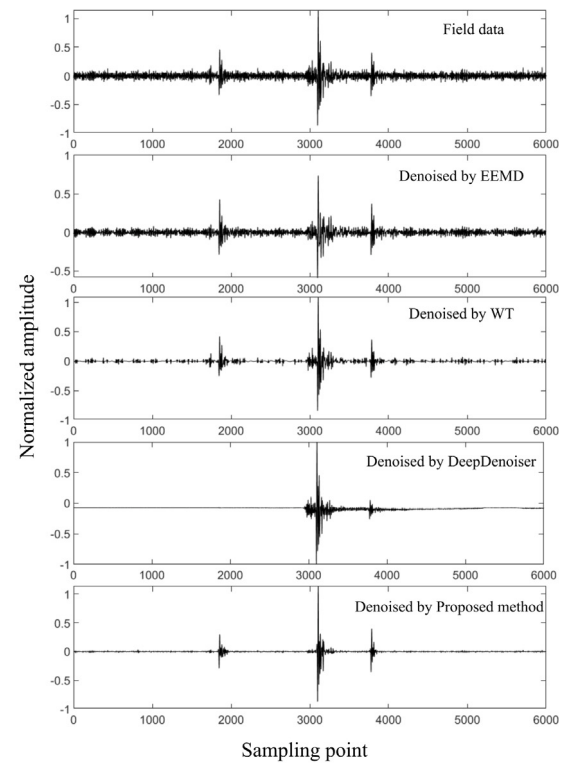


Fig. 15. The waveforms cut from the denoising results for data set 2.

signals, and significantly improve the SNR of noisy signals. Compared with the traditional denoising method, which only has an excellent performance to suppress linear noise, the proposed method has better adaptability, and also has an excellent performance to denoise complex

nonlinear real noise in different regions. Compared with DeepDenoiser, the proposed method has better signal retention and integrity, which can be well applied to the microseismic signal processing and signal analysis in the geophysical field.

Declaration of competing interest

The authors declare that they have no known competing financial interests or personal relationships that could have appeared to influence the work reported in this paper.

Funding

This work is financially supported in part by National Natural Science Foundation of China (42272204), the National Key Research and Development Program of China (2018YFB0605503), the Fundamental Research Funds for the Central Universities, China under Grant (2021JCCXDC02).

References

- Allen, J., Rabiner, L., 1977. A unified approach to short-time Fourier analysis and synthesis. Proc. IEEE 65 (11), 1558–1564. <http://dx.doi.org/10.1109/PROC.1977.10770>.
- Bekara, M., Baan, M., 2009. Random and coherent noise attenuation by empirical mode decomposition. Geophysics 74, V89–98. <http://dx.doi.org/10.1190/1.3157244>.
- Cao, S., Chen, X., 2005. The second-generation wavelet transform and its application in denoising of seismic data. Appl. Geophys. 2, 70–74. <http://dx.doi.org/10.1007/s11770-005-0034-4>.
- Chen, W., Xie, J., Zu, S., Shuwei, G., Chen, Y., 2016. Multiple-reflection noise attenuation using adaptive randomized-order empirical mode decomposition. IEEE Geosci. Remote Sens. Lett. PP, <http://dx.doi.org/10.1109/LGRS.2016.2622918>.
- Dai, L., Dong, H., Li, X., 2019. Review of microseismic data denoising methods. J. Jilin Univ.(Earth Sci. Ed.).
- Gaci, S., 2014. The use of wavelet-based denoising techniques to enhance the first-arrival picking on seismic traces. IEEE Trans. Geosci. Remote Sens. 52 (8), 4558–4563. <http://dx.doi.org/10.1109/TGRS.2013.2282422>.
- Galiana-Merino, J., Rosa-Herranz, J., Giner, J., Molina, S., Botella, F., 2003. De-noising of short-period seismograms by wavelet packet transform. Bull. Seismol. Soc. Am. 93, 2554–2562.
- Guo, S., Yan, Z., Zhang, K., Zuo, W., Zhang, L., 2019. Toward convolutional blind denoising of real photographs. In: 2019 IEEE/CVF Conference on Computer Vision and Pattern Recognition. CVPR, pp. 1712–1722. <http://dx.doi.org/10.1109/CVPR.2019.00181>.
- Han, J., Baan, M., 2015. Microseismic and seismic denoising via ensemble empirical mode decomposition and adaptive thresholding. Geophysics 80, KS69 – KS80. <http://dx.doi.org/10.1109/GEO2014-0423.1>.
- Kim, Y., Hardisty, R., Marfurt, K., 2019. Seismic random noise attenuation in f-x domain using complex-valued residual convolutional neural network. pp. 2579–2583. <http://dx.doi.org/10.1109/segam2019-3216543.1>.
- Li, H., Yang, W., Yong, X., 2018. Deep learning for ground-roll noise attenuation. pp. 1981–1985. <http://dx.doi.org/10.1109/segam2018-2981295.1>.
- Liu, W., Cao, S., Chen, Y., 2016. Seismic time-frequency analysis via empirical wavelet transform. IEEE Geosci. Remote Sens. Lett. 13 (1), 28–32. <http://dx.doi.org/10.1109/LGRS.2015.2493198>.
- Liu, Y., Li, Y., Lin, H., Ma, H., 2014. An amplitude-preserved time–frequency peak filtering based on empirical mode decomposition for seismic random noise reduction. Geosci. Remote Sens. Lett. IEEE 11, 896–900. <http://dx.doi.org/10.1109/LGRS.2013.2281202>.
- Liu, L., Song, W., Zeng, C., Yang, X., 2021. Microseismic event detection and classification based on convolutional neural network. J. Appl. Geophys. 192, 104380. <http://dx.doi.org/10.1016/j.jappgeo.2021.104380>, URL <https://www.sciencedirect.com/science/article/pii/S0926985121001270>.
- Liu, D., Wang, W., Chen, W., Wang, X., Zhou, Y., Shi, Z., 2018. Random-noise suppression in seismic data: What can deep learning do?. pp. 2016–2020. <http://dx.doi.org/10.1190/segam2018-2998114.1>.
- Mandelli, S., Lipari, V., Bestagini, P., Tubaro, S., 2019. Interpolation and denoising of seismic data using convolutional neural networks. CoRR abs/1901.07927, [arXiv:1901.07927](https://arxiv.org/abs/1901.07927).
- Mousavi, S.M., Langston, C.A., 2016a. Adaptive noise estimation and suppression for improving microseismic event detection. J. Appl. Geophys. 132, 116–124. <http://dx.doi.org/10.1016/j.jappgeo.2016.06.008>, URL <https://www.sciencedirect.com/science/article/pii/S092698511630163X>.
- Mousavi, S.M., Langston, C.A., 2016b. Hybrid seismic denoising using higher-order statistics and improved wavelet block thresholding. Bull. Seismol. Soc. Am. 106 (4), 1380–1393. <http://dx.doi.org/10.1785/0120150345>.
- Mousavi, S.M., Langston, C., 2017. Automatic noise-removal/signal-removal based on general cross-validation thresholding in synchrosqueezed domain and its application on earthquake data. Geophysics 82, 1–58. <http://dx.doi.org/10.1190/geo2016-0433.1>.
- Mousavi, S.M., Langston, C.A., Horton, S.P., 2016. Automatic microseismic denoising and onset detection using the synchrosqueezed continuous wavelet transform. Geophysics 81 (4), V341–V355. <http://dx.doi.org/10.1190/geo2015-0598.1>.
- Neelamani, R., Baumstein, A., Gillard, D., Hadidi, M., Soroka, W., 2008. Coherent and random noise attenuation using the curvelet transform. Geophysics 27, <http://dx.doi.org/10.1190/1.2840373>.
- Ronneberger, O., Fischer, P., Brox, T., 2015. U-net: Convolutional networks for biomedical image segmentation. CoRR abs/1505.04597, [arXiv:1505.04597](https://arxiv.org/abs/1505.04597).
- Sabbione, J., Sacchi, M., Velis, D., 2015. Radon transform-based microseismic event detection and signal-to-noise ratio enhancement. J. Appl. Geophys. 113, 51–63. <http://dx.doi.org/10.1016/j.jappgeo.2014.12.008>.
- Sabbione, J., Velis, D., Sacchi, M., 2013. Microseismic data denoising via an apex-shifted hyperbolic radon transform. pp. 2155–2161. <http://dx.doi.org/10.1190/segam2013-1414.1>.
- Shuchong, L., Xun, C., 2015. Seismic signals wavelet packet denoising method based on improved threshold function and adaptive threshold.
- Si, X., Yuan, Y., 2018. Random noise attenuation based on residual learning of deep convolutional neural network. pp. 1986–1990. <http://dx.doi.org/10.1190/segam2018-2985176.1>.
- Tselentis, G.-A., Martakis, N., Paraskevopoulos, P., Lois, A., Sokos, E., 2012. Strategy for automated analysis of passive microseismic data based on S-transform, Otsu's thresholding, and higher order statistics. Geophysics 77 (6), KS43–KS54. <http://dx.doi.org/10.1190/geo2011-0301.1>.
- Zhang, H., Ma, C., Pazzi, V., Zou, Y., Casagli, N., 2020. Microseismic signal denoising and separation based on fully convolutional encoder–decoder network. Appl. Sci. 10, 6621. <http://dx.doi.org/10.3390/app10186621>.
- Zhang, L., Wang, Y., Zheng, Y., Chang, X., 2015. Deblending using a high-resolution radon transform in a common midpoint domain. J. Geophys. Eng. 12, <http://dx.doi.org/10.1088/1742-2132/12/2/167>.
- Zhang, K., Zuo, W., Chen, Y., Meng, D., Zhang, L., 2017. Beyond a Gaussian denoiser: Residual learning of deep CNN for image denoising. IEEE Trans. Image Process. 26 (7), 3142–3155. <http://dx.doi.org/10.1109/TIP.2017.2662206>.
- Zheng, J., Jiang, T., Wu, Z., Sun, Y., 2021. Application of residual learning to microseismic random noise attenuation. Acta Geophys. 69, 1–11. <http://dx.doi.org/10.1007/s11600-021-00591-9>.
- Zhu, W., Mousavi, S.M., Beroza, G.C., 2019. Seismic signal denoising and decomposition using deep neural networks. IEEE Trans. Geosci. Remote Sens. 57 (11), 9476–9488. <http://dx.doi.org/10.1109/TGRS.2019.2926772>.